ACADÉMIE
DES SCIENCES
INSTITUT DE FRANCE

Comptes Rendus
Mécanique

Simeon Djambov and François Gallaire

Analytical solutions to the gravity-driven rain-fed free-surface Stokes equations

Volume 354 (2026), p. 451-459

Online since: 4 May 2026

https://doi.org/10.5802/crmeca.365

The Comptes Rendus. Mécanique *are a member of the Mersenne Center for open scientific publishing*
www.centre-mersenne.org — e-ISSN : 1873-7234

ACADÉMIE DES SCIENCES
INSTITUT DE FRANCE

Comptes Rendus. Mécanique
2026, Vol. 354, p. 451-459
https://doi.org/10.5802/crmeca.365

Research article

Analytical solutions to the gravity-driven rain-fed free-surface Stokes equations

Simeon Djambov [a, *, a, b] **and François Gallaire** [a, a]

[a] Laboratory of Fluid Mechanics and Instabilities, EPFL, Lausanne CH-1015, Switzerland

[b] LadHyX, CNRS, École Polytechnique, Institut Polytechnique de Paris, 91128 Palaiseau cedex, France

E-mails: simeon.djambov@epfl.ch, francois.gallaire@epfl.ch

Abstract. The present paper concerns the continuously-fed, gravity-driven film flows of rainwater over hemispheres and semicircular cylinders. We extend previous lubrication results to arbitrarily thick films, while remaining in the creeping flow limit. We show that the predictions of uniform thickness profiles, amusingly, remain qualitatively accurate under these relaxed assumptions.

Keywords. Thin film, free surface, rain.

Funding. We acknowledge the Swiss National Science Foundation under grant #10001049. Some of this work was carried out while S.D. was hosted by Sylvain Courrech du Pont at Laboratoire Matière et Systèmes Complexes in Paris, and partially supported by an EPFL Doc.Mobility grant.

Manuscript received 4 February 2026, revised and accepted 27 April 2026, online since 4 May 2026.

1. Introduction

Thin-film flows are ubiquitous in both natural and industrial settings, and their theoretical description has received particular attention and continued research efforts [1]. The endeavour of lubrication theory resides in taking advantage of a scale separation between the film thickness and other length scales, such as a characteristic length of the topography, and performing some kind of depth integration, in order to reduce the dimensionality of the problem. The interaction of different physical processes, possibly at play, and topographical geometry has served as a boundless playground. A recent example can be found in the effort of Ledda et al. (2022), applying tools from differential geometry towards the modelling of coating flows over arbitrarily curved substrates [2].

Geometries, which attract notable interest thanks to their simplicity, are the sphere and the cylinder. At a fixed liquid volume, if the coating flow's advancing contact line does not break up into fingers [3,4], the coating layer could reach a steady profile [5,6], which could further destabilise into droplets in the case of the horizontally axed cylinder [7]. In the case of continuously fed film flows, Gyure & Krantz (1983) studied the steady film flow around a sphere from a point source at the pole [8], while in his pioneering work on filmwise condensation Nusselt (1916) considered not only inclined planes, but also horizontal cylinders [9].

* Corresponding author

Besides condensation, another natural occurrence of a spatially distributed source is rainfall. Concerned with transmission losses due to rainwater film flows over the spherical protection shells around radars, known as radomes, Gibble (1964) found a uniform rain-fed film thickness, through a lubrication argument [10]. Recently, Guo & Mei (2019) revisited Gibble's result by considering texture-induced slip, a technique commonly used for the purpose of reducing transmission losses by making the rainwater film thinner [11]. They examined a square lattice of circular pillars and solved full Navier–Stokes microscopic problems at different polar stations: obtaining the local slip length at each station and updating the macroscopic flow in a lubrication setting enabled them to set up an iterative scheme, converging to a non-uniform film thickness profile.

Interested in rainwater runoff on roads, Becker (1975) obtained a uniform thickness on cylindrical surfaces, also in a thin-film context [12]. He considered both inertial effects and effective dynamic pressure and shear stress from raindrop impacts, which, remarkably, did not alter the prediction of a uniform thickness; furthermore, the associated corrections were shown to be non-essential for realistic applications.

Here, we address cases where inertia (both of the raindrops and of the film) is negligible and focus on the upper halves of spheres and cylinders. Under these hypotheses, we show that the thin-film assumption of previous studies can be relaxed and obtain exact solutions to the full free-surface Stokes equations. We leverage the classical Stokes flow around a sphere and circular cylinder [13], which can strikingly be adapted to satisfy all the boundary conditions and the volume conservation. We further show that the lubrication results remain correct, as compared with the full Stokes solution, up to film thicknesses of the order of the radius of curvature.

2. Problem formulation

Consider the gravity-driven viscous film flow of a Newtonian liquid (water) with density ρ, kinematic viscosity ν, and surface tension γ, fed by a continuous, uniform, downward-oriented vertical volumetric flux q — an idealised "rainfall". All material properties are considered constant. What is then the stationary, azimuthally (respectively axially) invariant thickness profile $h(\theta)$ over a hemisphere (respectively horizontally axed semi-circular cylinder) of radius R (Figure 1)?

All lengths are rescaled with R, the pressure $p(r,\theta)$ is made dimensionless using a hydrostatic scale $\rho g R$, while the velocity $\boldsymbol{u}(r,\theta)$ is non-dimensionalised using a viscous-gravity scale gR^2/ν, where g is the magnitude of the gravitational acceleration. This naturally leads to a dimensionless rainfall rate $\mathrm{Q} = \nu q/(gR^2)$. The dimensionless incompressible Stokes equations read

$$\boldsymbol{\nabla}\cdot\boldsymbol{u} = 0, \tag{1}$$

$$\boldsymbol{\nabla}\cdot\boldsymbol{\Sigma} - \hat{\boldsymbol{z}} = \boldsymbol{0}, \tag{2}$$

with the stress tensor $\boldsymbol{\Sigma} = -p\boldsymbol{I} + (\boldsymbol{\nabla}\boldsymbol{u} + \boldsymbol{\nabla}\boldsymbol{u}^T)$ and the upward-pointing vertical unit-vector $\hat{\boldsymbol{z}} = \cos\theta\hat{\boldsymbol{r}} - \sin\theta\hat{\boldsymbol{\theta}}$. General wall boundary conditions, which may include slip and interfacial transpiration for rough surfaces, read

$$u_\theta(r=1,\theta) = \lambda\boldsymbol{\Sigma}_{r\theta} + \frac{\mathscr{K}^{\mathrm{itf}}}{r}\frac{\partial\boldsymbol{\Sigma}_{rr}}{\partial\theta}\bigg|_{r=1}, \tag{3a}$$

$$u_r(r=1,\theta) = -\frac{\mathscr{K}^{\mathrm{itf}}}{r}\frac{\partial\boldsymbol{\Sigma}_{r\theta}}{\partial\theta}\bigg|_{r=1}, \tag{3b}$$

with the dimensionless slip length λ and interfacial permeability $\mathscr{K}^{\mathrm{itf}}$, assumed spatially uniform [14–16]. This is a second-order homogenised boundary condition, only recently applied to thin-film flows, for the case of Landau–Levich dip coating [16].

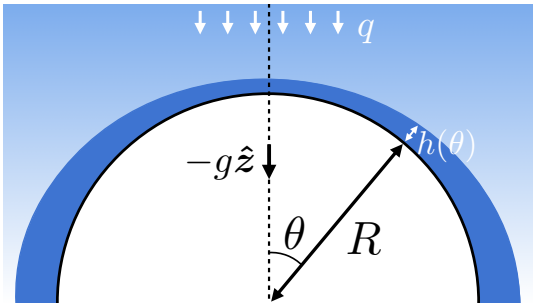

Figure 1. Sketch of the problem at hand.

The liquid-air interface is assumed free of tangential stresses and undergoing a curvature-induced Laplace jump in the normal stress,

$$\boldsymbol{\Sigma}\,\hat{\boldsymbol{n}} + \mathrm{We}(\boldsymbol{\nabla}\cdot\hat{\boldsymbol{n}})\hat{\boldsymbol{n}}\big|_{r=1+h} = 0, \tag{4}$$

with the Weber number $\mathrm{We} = \gamma/(\rho g R^2)$ and the outward-pointing unit-vector, normal to the interface,

$$\hat{\boldsymbol{n}} = \left.\frac{\boldsymbol{\nabla}[r-h]}{\|\boldsymbol{\nabla}[r-h]\|}\right|_{r=1+h}. \tag{5}$$

Finally, the rain film's thickness profile is governed by the conservation of liquid volume or, equivalently, a kinematic boundary condition.

3. Hemisphere

The steady flow rate through the film at any polar position θ is the accumulation of the captured rain, i.e. the product of the rainfall rate and the area of the disk of radius, equal to the projected radial position of the free surface at θ; and the eventual interfacial transpiration from the rough wall, eq. (3b),

$$2\pi\sin\theta\int_1^{1+h(\theta)} u_\theta(r,\theta)\,r\,\mathrm{d}r = \pi\sin^2\theta\big(1+h(\theta)\big)^2\mathrm{Q} + 2\pi\int_0^\theta u_r(r=1,\theta)\sin\theta\,\mathrm{d}\theta. \tag{6}$$

Observe that if ever the polar velocity $u_\theta(r,\theta)$ is separable as the product of $\sin\theta$ and any function of r, then, according to the continuity equation (1), $u_r(r=1,\theta)$ would behave as $\cos\theta$ and the explicit polar dependence would cancel in all terms of the above equation, which means that the thickness profile could be uniform, $h(\theta) = h_s = \text{const}$. This leads to an ansatz for a divergence-free velocity field and for the pressure field of the form

$$u_\theta(r,\theta) = \frac{\psi'(r)\sin\theta}{2r}, \qquad u_r(r,\theta) = -\frac{\psi(r)\cos\theta}{r^2}, \qquad p(r,\theta) = p_0 + f(r)\cos\theta, \tag{7}$$

where primes $'$ indicate differentiation. Notice that this velocity profile has the exact form as that of Stokes flow past a sphere, with a streamfunction [13, p. 52]

$$\Psi(r,\theta) = \frac{\psi(r)\sin^2\theta}{2}. \tag{8}$$

The pressure profile is obtained from the polar component of the Stokes equations (2),

$$f(r) = -r - \frac{2\psi(r)}{r^3} + \frac{\psi'(r)}{r^2} - \frac{\psi'''(r)}{2}, \tag{9}$$

while the radial component reduces to an equidimensional ordinary differential equation, i.e. invariant to the scale change $r \to mr$ [17, p. 12],

$$r^4\psi''''(r) - 4r^2\psi''(r) + 8r\psi'(r) - 8\psi(r) = 0 \tag{10}$$

with the well-known general solution,

$$\psi(r) = \frac{s_1}{r} + s_2 r + s_3 r^2 + s_4 r^4. \tag{11}$$

The four constants of integration s_i are obtained by imposing the wall boundary conditions (3),

$$u_\theta(r=1,\theta) = \lambda\left(r\frac{\partial(u_\theta/r)}{\partial r} + \frac{1}{r}\frac{\partial u_r}{\partial\theta}\right) + \frac{\mathcal{K}^{\mathrm{itf}}}{r}\left(-\frac{\partial p}{\partial\theta} + 2\frac{\partial^2 u_r}{\partial r\partial\theta}\right)\Bigg|_{r=1}$$

$$\iff \quad \frac{\psi'(1)}{2} = \lambda\left(\psi(1) - \psi'(1) + \frac{\psi''(1)}{2}\right) - \mathcal{K}^{\mathrm{itf}}\left(1 + 6\psi(1) - 3\psi'(1) + \frac{\psi'''(1)}{2}\right), \tag{12a}$$

$$u_r(r=1,\theta) = -\frac{\mathcal{K}^{\mathrm{itf}}}{r}\left(r\frac{\partial^2(u_\theta/r)}{\partial r\partial\theta} + \frac{1}{r}\frac{\partial^2 u_r}{\partial\theta^2}\right)\Bigg|_{r=1} \quad \iff \quad \psi(1) = \mathcal{K}^{\mathrm{itf}}\left(\psi(1) - \psi'(1) + \frac{\psi''(1)}{2}\right), \tag{12b}$$

and the free-surface dynamic boundary conditions (4),

$$r\frac{\partial(u_\theta/r)}{\partial r} + \frac{1}{r}\frac{\partial u_r}{\partial\theta}\bigg|_{r=1+h_s} = \sin\theta\left\{\frac{\psi(r)}{r^3} - \frac{\psi'(r)}{r^2} + \frac{\psi''(r)}{2r}\right\}\bigg|_{r=1+h_s} = 0, \tag{13a}$$

$$-p + 2\frac{\partial u_r}{\partial r}\bigg|_{r=1+h_s} = \cos\theta\left\{r + \frac{6\psi(r)}{r^3} - \frac{3\psi'(r)}{r^2} + \frac{\psi'''(r)}{2}\right\}\bigg|_{r=1+h_s} - p_0 = -\frac{2\mathrm{We}}{1+h_s}. \tag{13b}$$

All of the above conditions are satisfied for $p_0 = 2\mathrm{We}/(1+h_s)$ and

$$s_1 = \frac{(1+h_s)^5\left[(1+h_s)^3(1-6\mathcal{K}^{\mathrm{itf}}) + 6\mathcal{K}^{\mathrm{itf}}\right]}{3\left[(1+h_s)^5\left(3+6\lambda-18\mathcal{K}^{\mathrm{itf}}\right) + 2 - 6\lambda + 18\mathcal{K}^{\mathrm{itf}}\right]}, \tag{14a}$$

$$s_2 = -\frac{(1+h_s)^3}{3}, \tag{14b}$$

$$s_3 = -s_2 + (3\mathcal{K}^{\mathrm{itf}} - 1)(s_1 + s_4), \tag{14c}$$

$$s_4 = -\frac{s_1}{(1+h_s)^5}. \tag{14d}$$

Finally, the film thickness h_s is determined by the condition (6),

$$\psi(r = 1+h_s) = (1+h_s)^2\mathrm{Q}. \tag{15}$$

Note that this is equivalent to the kinematic condition $u_r(r = 1+h_s,\theta) = -\mathrm{Q}\cos\theta$. While the above relation is implicit in $h_s(\mathrm{Q})$, it is explicit in $\mathrm{Q}(h_s)$.

Keeping in mind that λ and $\mathcal{K}^{\mathrm{itf}}$ result from a first- and second-order homogenisation procedure [15], one can assume that they are at most $\mathcal{O}[h_s]$ and $\mathcal{O}[h_s^2]$, respectively. An expansion for small $h_s \ll 1$ then reads

$$\mathcal{K}^{\mathrm{itf}}h_s + 2\lambda h_s^2 + \frac{2}{3}h_s^3 + \mathcal{O}[h_s^4] = \mathrm{Q}. \tag{16}$$

It differs from the lubrication model used by Guo & Mei (2019) [11] by the first term, linear in h_s, introduced by the interfacial transpiration and which qualitatively modifies the asymptotic behaviour for small h_s. It is worth pointing out that the lubrication equation, derived by Molefe et al. (2024), also presents a term linear in the thickness, due to interfacial transpiration [16].

In the case of smooth spheres, $\lambda = \mathcal{K}^{\mathrm{itf}} = 0 = \psi(1)$, where the film thickness shall be denoted with a capital H_s, the full solution reads

$$\psi(r) = \frac{(1+H_s)^3 r(r-1)}{3} - \frac{(1+H_s)^3}{6+9(1+H_s)^5}\left\{\frac{(1+H_s)^5}{r}(r^3-1) + r^2(r^2-1)\right\}, \tag{17}$$

with

$$\mathrm{Q} = \frac{\psi(r=1+H_s)}{(1+H_s)^2} = \frac{H_s(1+H_s)^2}{3} - \frac{(1+H_s)^3\big((1+H_s)^5-1\big)}{6+9(1+H_s)^5} = \frac{2H_s^3}{3} + \mathscr{O}[H_s^4], \tag{18}$$

where Gibble's (1964) result is retrieved asymptotically for small H_s [10].

4. Semi-circular cylinder

In the cylindrical geometry, the conservation of liquid volume instead reads

$$\int_1^{1+h(\theta)} u_\theta(r,\theta)\,\mathrm{d}r = \sin\theta\big(1+h(\theta)\big)\mathrm{Q} + \int_0^\theta u_r(r=1,\theta)\,\mathrm{d}\theta. \tag{19}$$

In perfect analogy to the spherical case, the ansatz

$$u_\theta(r,\theta) = \psi'(r)\sin\theta, \qquad u_r(r,\theta) = -\frac{\psi(r)\cos\theta}{r}, \qquad p(r,\theta) = p_0 + f(r)\cos\theta, \tag{20}$$

satisfies the continuity equation (1) and admits a uniform thickness profile $h(\theta) = h_c = \text{const}$. Once more, these share the form of Stokes flow past a circular cylinder with a streamfunction $\Psi(r,\theta) = \psi(r)\sin\theta$, and with the well-known general solution [13, p. 55]

$$\psi(r) = \frac{c_1}{r} + c_2 r + c_3 r\ln r + c_4 r^3. \tag{21}$$

The pressure's radial profile instead reads

$$f(r) = -r - \frac{2\psi(r)}{r^2} + \frac{2\psi'(r)}{r} - \psi''(r) - r\psi'''(r). \tag{22}$$

The boundary conditions at the wall (3) become

$$\psi'(1) = \lambda\big(\psi(1) - \psi'(1) + \psi''(1)\big) - \mathscr{K}^{\mathrm{itf}}\big(1 + 4\psi(1) - 4\psi(1) + \psi''(1) + \psi'''(1)\big), \tag{23a}$$

$$\psi(1) = \mathscr{K}^{\mathrm{itf}}\big(\psi(1) - \psi'(1) + \psi''(1)\big), \tag{23b}$$

while the free-surface dynamic boundary conditions (4) produce

$$\left.\frac{\psi(r)}{r^2} - \frac{\psi'(r)}{r} - \psi''(r)\right|_{r=1+h_c} = 0, \tag{24a}$$

$$\left. r + \frac{4\psi(r)}{r^2} - \frac{4\psi'(r)}{r} + \psi''(r) + r\psi'''(r)\right|_{r=1+h_c} = 0, \qquad p_0 = \frac{\mathrm{We}}{1+h_c}. \tag{24b}$$

These constraints determine the coefficients c_i,

$$c_1 = \frac{(1+h_c)^4\big[(1+h_c)^2(1-4\mathscr{K}^{\mathrm{itf}}) + 4\mathscr{K}^{\mathrm{itf}}\big]}{8\big[(1+h_c)^4(1+2\lambda-4\mathscr{K}^{\mathrm{itf}}) + 1 - 2\lambda + 4\mathscr{K}^{\mathrm{itf}}\big]}, \tag{26a}$$

$$c_2 = (4\mathscr{K}^{\mathrm{itf}} - 1)(c_1 + c_4), \tag{26b}$$

$$c_3 = \frac{(1+h_c)^2}{4}, \tag{26c}$$

$$c_4 = -\frac{c_1}{(1+h_c)^4}. \tag{26d}$$

Analogously to the sphere, the film thickness is obtained by the condition (19),

$$\psi(r=1+h_c) = (1+h_c)\mathrm{Q}. \tag{27}$$

An expansion of the above relation for small $h_c \ll 1$, with $\lambda = \mathscr{O}[h_c]$ and $\mathscr{K}^{\mathrm{itf}} = \mathscr{O}[h_c^2]$, reads

$$\mathscr{K}^{\mathrm{itf}} h_c + \lambda h_c^2 + \frac{1}{3}h_c^3 + \mathscr{O}[h_c^4] = \mathrm{Q}. \tag{28}$$

In the case of smooth cylinders, $\lambda = \mathscr{K}^{\mathrm{itf}} = 0 = \psi(1)$, the solution reads

$$\psi(r) = \frac{(1+H_c)^2 r\ln r}{4} - \frac{(1+H_c)^2(r^2-1)\big[(1+H_c)^4 + r^2\big]}{8\big(1+(1+H_c)^4\big)r}, \tag{29}$$

with

$$\begin{aligned} \mathrm{Q} &= \frac{\psi(r=1+H_c)}{(1+H_c)} \\ &= \frac{(1+H_c)^2\ln[1+H_c]}{4} - \frac{H_c(2+H_c)(1+H_c)^2\left(1+(1+H_c)^2\right)}{8+8(1+H_c)^4} = \frac{H_c^3}{3} + \mathscr{O}[H_c^4], \end{aligned} \tag{30}$$

where the asymptotic behaviour for small H_c also coincides with the prediction from lubrication theory [12].

5. Results

A visualisation of a sample rain film flow around a smooth spherical dome, eq. (17), and circular arch, eq. (29), is presented in Figure 2. Observe first that the film over the horizontal cylinder (left) is thicker than the one over the sphere (right). A shared colormap encodes for the velocity magnitude, while iso-contours of the streamfunction trace out the streamlines (at levels, shared between the sphere and the cylinder). Keeping in mind that the volumetric flux between two streamlines is equal to the difference between the streamfunction, evaluated on each of them [18], notice how the divergent flow near the sphere's pole "repulses" the first streamlines further away from the wall, compared to the cylinder.

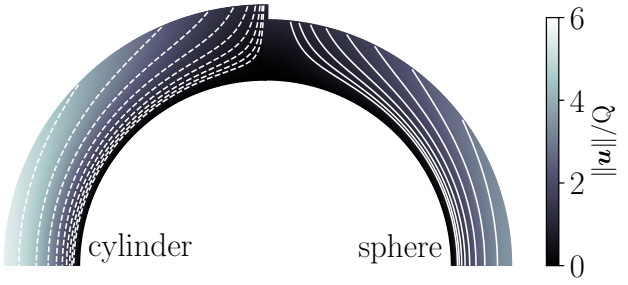

Figure 2. Heatmap of the velocity magnitude, normalised by the rainfall rate (shared colorbar). Streamlines: iso-contours of the streamfunction at shared levels, around the smooth cylinder (left, dashed lines) and sphere (right, solid lines). Here, $\mathrm{Q} = 0.02$ and $\lambda = \mathscr{K}^{\mathrm{itf}} = 0$. This corresponds to dimensionless film thicknesses $H_c \approx 0.39$ and $H_s \approx 0.31$.

Figure 3 represents the film thicknesses $H_{s,c}$ over smooth spheres, eq. (18), and cylinders, eq. (30), as a function of the dimensionless rainfall rate Q. As expected, deviations from the asymptotic, thin-film behaviours are only observed once the thicknesses become comparable to the radius of curvature, $H_{s,c} \approx 1$. In fact, the lubrication approximation then underestimates the film thickness. This is the result of two competing effects: for thick films, (i) the full Stokes flow presents a deformed half-Poiseuille velocity profile (see Figure 4); it turns out that the flow rate increases faster than $H_{s,c}^3$, which means that for a given flow rate, the films do not need to be as thick as predicted by lubrication theory; however, (ii) thick films contribute to the capturing of more rain (factors of $\left(1+h(\theta)\right)^2$ on the right-hand side of eq. (6) and $\left(1+h(\theta)\right)$ in eq. (19)). On the sphere, these two effects balance and the large-H_s behaviour remains proportional to $\mathrm{Q}^{1/3}$ (with a different prefactor of $(9/2)^{1/3}$ rather than $(3/2)^{1/3}$), while on the cylinder, H_c continues to grow ever faster than $\mathrm{Q}^{1/3}$.

Figure 5 shows the effect of roughness on the rain film thickness in the thin-film limits, eqs. (16) and (28). Indeed, only films of thickness commensurate with the slip length — which is of the order of the roughness and, thus, necessarily much smaller than the radius R — may experience a significant effect. Molefe et al. (2024) recently reported that $\mathscr{K}^{\mathrm{itf}} \approx \lambda^2$ for a

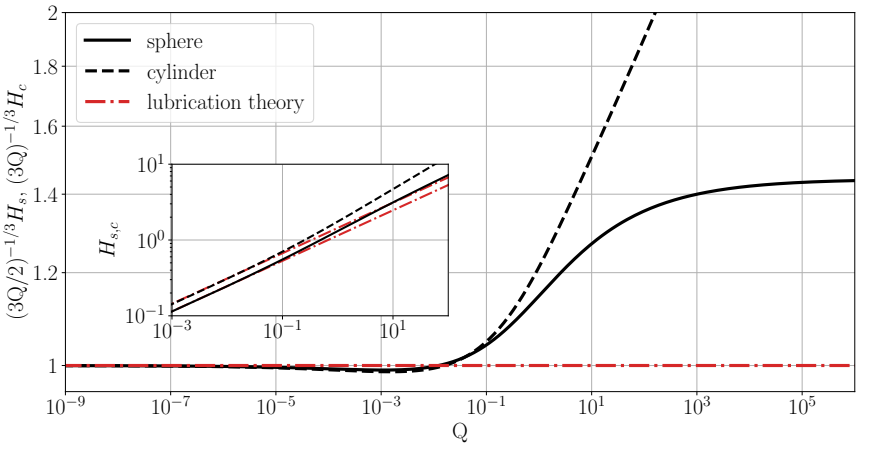

Figure 3. Dimensionless film thickness $H_{s,c}$ (inset), rescaled by the lubrication results (main panel), as a function of the dimensionless rainfall rate Q for the smooth cases, eqs. (18) and (30), $\lambda = \mathcal{K}^{\text{itf}} = 0$. The red dash-dotted lines depict the asymptotic behaviours predicted by lubrication theory.

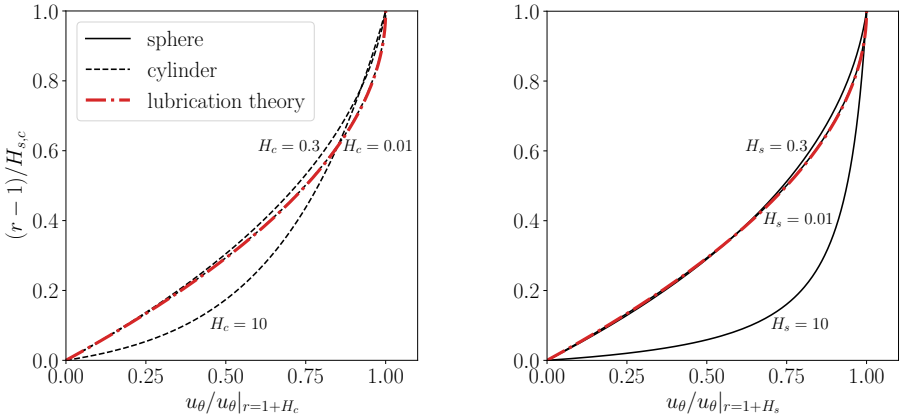

Figure 4. Polar velocity profile, normalised by the free-surface polar velocity, across the thickness of the rain film over a smooth cylinder (left panel) and sphere (right panel) for different film thicknesses $H_{s,c} = \{0.01, 0.3, 10\}$. The half-Poiseuille lubrication profile is displayed in red dash-dotted lines.

wide variety of micro-structures (pillars of different widths and heights, upright and inverted cones) [16]. This implies in eqs. (16) and (28) that $h_{s,c}/H_{s,c}$ is a function only of $\lambda/H_{s,c}$, where we remind that the lower (respectively, upper) case stands for the rough (respectively, smooth) case. We observe that the thinning is relatively more important on cylinders than on spheres. By contrast, ignoring the second-order effect of interfacial transpiration ($\mathcal{K}^{\text{itf}} = 0$, grey line) as did, for example, Guo & Mei (2019) [11] makes the two cases identical, while leading to an underestimation of the thinning effect.

6. Conclusion

We have shown that the lubrication predictions for uniform rain-fed films on spherical domes and circular arches [10,12] still hold, qualitatively, in a free-surface Stokes flow setting, despite relaxing the assumption that the film thickness should be much smaller than the radius of

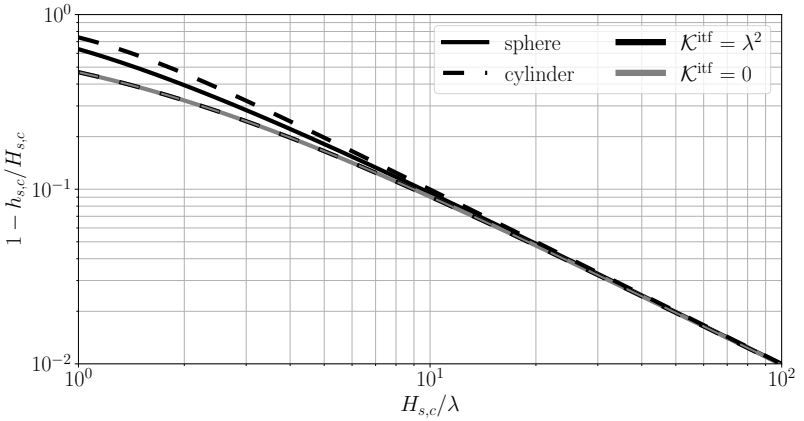

Figure 5. Roughness-induced thinning, eqs. (16) and (28), with (black lines) and without (grey lines) interfacial transpiration. Note that without interfacial transpiration, the spherical and cylindrical cases are identical.

curvature. This is thanks to a coincidental compatibility between the flow rate's polar evolution of the classical Stokes flows past spheres and circular cylinders and the polar evolution of these geometries' projected area.

The solution around the cylinder is noteworthy for another reason as well: in contrast to the paradoxical non-existence of Stokes flow past a cylinder in an infinite domain [13], here the solution is useful as a result of the finitude of the domain. It is also valuable to mention that, as already observed by Becker (1975), the two-dimensional film flow over a horizontally axed circular cylinder can be straightforwardly generalised to inclined cylinders: the axial velocity u_z would remain decoupled from the already obtained velocity field and would be a solution to Poisson's equation [12].

Moreover, we have verified that the lubrication predictions remain quantitatively accurate as well, as long as the film thickness is smaller than the radius of curvature, which was expected. While the scale separation is by far not the first assumption that would fail — effective stresses from the raindrop impacts and inertia are expected to become important much earlier — our hope is for this analytical solution to serve as possible validation of direct numerical simulations of free-surface flows, which are notoriously challenging, or to new depth-integrated models, which strive to extend the domain of validity in separation of scales.

We have also shown that interfacial transpiration accounts for a significant part of the roughness-induced thinning. Its crucial importance was already noted by Molefe et al. (2024) for their dip-coating study, where its addition led to a qualitatively different prediction, confirmed by their experiments [16].

Lastly, it should be emphasised that while the present solution confirms lubrication theory results in its thin-film limit, its applicability for thicker films depends profoundly on the outflow boundary condition. In the volume conservation equations (6) and (19), we have implicitly symmetrised the problem around the equator. If, for example, one considers complete spheres and cylinders, the accumulated rainwater flow rate (first term on the right-hand side of eqs. (6) and (19)) should remain constant for $\theta > \pi/2$, rather than decrease with θ. This would require matching a rain-fed film flow on the upper hemisphere (respectively, semi-cylinder) to a constant flow rate film flow down the lower one. In the thin-film limit, the thickness profile for $\theta > \pi/2$ would behave as $\sin^{-2/3}\theta$ [8] (respectively, $\sin^{-1/3}\theta$ for the cylinder), and the matching would be immediate. Concerning thicker films however, not much can be intuited about the extent to which our present solution may remain relevant when matched with a generic outflow region.

Various scenarios can be imagined, ranging from the formation of a jet (or, respectively, a curtain) from the lowest point of the sphere (respectively, cylinder), to the deflection of the rainwater around supporting structures, e.g. a rod, or even the infiltration of the rainwater into the porous ground at the base of the sphere (or cylinder). All of these scenarios fall outside the scope of the present manuscript, as each of them requires special care in the connection with the uniform solution, described here.

Acknowledgments

We gratefully acknowledge Giuseppe A. Zampogna for his input on the general form of the rough wall boundary conditions. We would also like to thank John R. Lister for the insightful discussion following the Ph.D. defense of S.D. We thank the anonymous reviewer for finding a major error in the volume conservation equations.

Declaration of interests

The authors do not work for, advise, own shares in, or receive funds from any organization that could benefit from this article, and have declared no affiliations other than their research organizations.

References

[1] A. Oron, S. H. Davis and S. G. Bankoff, "Long-scale evolution of thin liquid films", *Rev. Mod. Phys.* **69** (1997), no. 3, pp. 931–980.
[2] P. G. Ledda, M. Pezzulla, E. Jambon-Puillet, P.-T. Brun and F. Gallaire, "Gravity-driven coatings on curved substrates: a differential geometry approach", *J. Fluid Mech.* **949** (2022), article no. A38 (36 pages).
[3] D. Takagi and H. E. Huppert, "Flow and instability of thin films on a cylinder and sphere", *J. Fluid Mech.* **647** (2010), pp. 221–238.
[4] G. Balestra, M. Badaoui, Y. M. Ducimetière and F. Gallaire, "Fingering instability on curved substrates: optimal initial film and substrate perturbations", *J. Fluid Mech.* **868** (2019), pp. 726–761.
[5] J. Qin, Y. T. Xia and P. Gao, "Axisymmetric evolution of gravity-driven thin films on a small sphere", *J. Fluid Mech.* **907** (2021), article no. A4 (18 pages).
[6] B. Reisfeld and S. G. Bankoff, "Non-isothermal flow of a liquid film on a horizontal cylinder", *J. Fluid Mech.* **239** (1992), pp. 167–196.
[7] S. Eghbali, S. Djambov and F. Gallaire, "Stability of a liquid layer draining around a horizontal cylinder: Interplay of capillary and gravity forces", *Phys. Rev. Fluids* **9** (2024), no. 6, article no. 063903 (17 pages).
[8] D. C. Gyure and W. B. Krantz, "Laminar film flow over a sphere", *Ind. Eng. Chem. Fundamen.* **22** (1983), no. 4, pp. 405–410.
[9] W. Nusselt, "Die Oberflächenkondensation des Wasserdampfes", *Z. Ver. Dtsch. Ing.* **60** (1916), pp. 541–546.
[10] D. Gibble, "Effect of rain on transmission performance of a satellite communication system", in *1964 IEEE International Convention Record*, IEEE International Convention Record, vol. 12, IEEE Press, 1965.
[11] X. Guo and C. C. Mei, "Liquid film on a hydrophobic radome or roof top in rain", *J. Fluid Mech.* **870** (2019), pp. 1158–1174.
[12] E. Becker, "Laminar film flow on a cylindrical surface", *J. Fluid Mech.* **74** (1975), no. 2, pp. 297–315.
[13] H. Ockendon and J. R. Ockendon, *Viscous Flow*, Cambridge University Press, 1995.
[14] G. A. Zampogna, J. Magnaudet and A. Bottaro, "Generalized slip condition over rough surfaces", *J. Fluid Mech.* **858** (2019), pp. 407–436.
[15] A. Bottaro and S. B. Naqvi, "Effective boundary conditions at a rough wall: a high-order homogenization approach", *Meccanica* **55** (2020), no. 9, pp. 1781–1800.
[16] L. Molefe, G. A. Zampogna, J. M. Kolinski and F. Gallaire, "Coating thickness prediction for a viscous film on a rough plate", *J. Fluid Mech.* **1001** (2024), article no. A59 (31 pages).
[17] C. M. Bender and S. A. Orszag, *Advanced Mathematical Methods for Scientists and Engineers*, McGraw-Hill, 1978.
[18] G. K. Batchelor, *An Introduction to Fluid Dynamics*, Cambridge University Press, 2000.